Performance of a quasi-synchronous four-dimensional super-orthogonal WCDMA modulator for next generation wireless applications

L.P. Linde*‡, L. Staphorst* and J.D. Vlok*

This paper presents the bit-error-rate (BER) performance of an upwards-expandable spectral and power efficient quasi-synchronous multi-layer-modulated (MLM) four-dimensional super-orthogonal wideband code-division multiple access (QS-4D-SO-WCDMA) modem, suitable for application in next generation WLAN and wireless cellular systems. The unique combination of the 4D-WCDMA modem configuration and super-orthogonal families of root-of-unity filtered (RUF) constant-envelope generalized-chirp-like complex spreading sequences (SO-CE-GCL-CSS), renders a spectrally and power efficient output signal with data throughput rates equivalent to that of a 16-ary quadrature amplitude modulated (16-QAM) WCDMA modulation scheme, but with the BER performance equivalent to that of BPSK/QPSK in both AWGN and fading multipath channel scenarios.

Introduction

The success whereby variants of multi-carrier orthogonal frequency division multiplexing (M_c-OFDM), including M_c-CDMA, have been introduced in WLAN standards such as 802.11a and g (WiFi), as well as in broadband wireless access standards such as 802.16-2004 (WiMax), has spawned the idea of extending their application to next generation single-carrier wireless cellular systems that have been based primarily on WCDMA modulation.

The spectral efficiency and data throughput advantages that M_c-OFDM-related modulation schemes exhibit over existing 3G single-carrier UMTS and WCDMA-2000 modulation standards are hampered, however, by the weak power efficiency of the former schemes, as manifested by their high peak-to-average power ratios (PAPR), as well as their sensitivity to mobility and fast fading.

The high OFDM PAPR requires power amplifier (PA) back-offs of typically 6 to 9 dBs to prevent signal amplitude saturation and corresponding spectral regrowth,[1,2] resulting in limited communication range due to inefficient utilization of available handset battery power. The OFDM performance and power inefficiency is further jeopardized by the use of multi-quadrature amplitude modulation (M-QAM) of individual orthogonal subcarriers in an effort to achieve improved spectral efficiency.[3] The performance degradation due to the use of these modulation schemes cannot be neutralized or improved without the inclusion of sophisticated forward error correction (FEC) and/or PAPR control coding mechanisms. This paper proposes an alternative low-complexity, upwards-expandable generic single carrier ($M_c = 1$) QS-4D-SO-WCDMA multi-layered-modulation (MLM) scheme with the potential to overcome the PAPR problems (even with $M_D \geq 4$ dimensions), while achieving significant BER performance gains which are QPSK-like, compared to single-carrier and M_c-OFDM and M_c-CDMA M-QAM modulation standards. The BER performances of the latter systems degrade significantly compared to QPSK, when the number of signal levels (or symbols) increases beyond $M_L = 4$ (i.e. $M = 16$).

*Department of Electrical, Electronic and Computer Engineering, University of Pretoria, Pretoria 0002, South Africa.
‡Author for correspondence. E-mail: llinde@postino.up.ac.za

Quasi-synchronous multi-code multi-dimensional super-orthogonal WCDMA

The new QS-4D-SO-WCDMA modem building block, depicted in Fig. 1, and the use of unique extended families of root-of-unity-filtered (RUF)[4] constant-envelope generalized chirp-like[5] complex spreading sequences (CE-GCL-CSS), exhibiting zero periodic and a-periodic cross-correlation (ZCC) values for all relative time shifts τ[6,7] [henceforth referred to as super-orthogonal (SO) sequences], together render a novel minimum (Nyquist) bandwidth near-constant envelope (or instantaneous power) output signal, while simultaneously facilitating multi-user-interference (MUI) free detection, even in the presence of rapidly varying multipath fading channel conditions.[8] This enables the use of significantly simplified correlation-type receiver structures without the need for complex MUI-cancellation mechanisms or sophisticated PAPR control measures normally required for M_c-OFDM-based systems. Whereas OFDMA schemes achieves multi-dimensionality and improved spectral efficiency (in bits s^{-1} Hz^{-1}) via a fixed set of M_c mutually orthogonal quadrature subcarriers and M-QAM modulation per subcarrier, single-carrier QS-4D-SO-WCDMA achieves multi-dimensionality and improved spectral efficiency through a multi-code MLM modulation approach, comprising the superposition of combinations of the point-by-point orthogonal real and imaginary parts* of sets of RUF SO-CE-GCL-CSS of length L chips, and the quadrature components of a carrier, which are individually binary phase and frequency, and optionally, also

*The real and imaginary components of each RUF CE-GCL-CSS are in fact Hilbert transforms of one another.

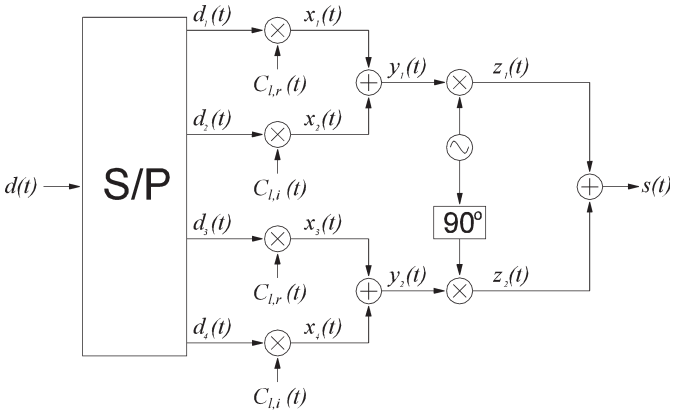

Fig. 1. Uncoded basic quasi-synchronous 4-dimensional super-orthogonal wideband code division multiple access (QS-4D-SO-WCDMA) modem transmitter building block.

Table 1. Uncoded performance comparison of MD-SO-WCDMA and *M*-QAM WCDMA modulation schemes in AWGN. To facilitate direct comparison, equal spreading sequence length *L* and spreading bandwidths B_s are assumed in each case.

Modulation scheme	Number of dimensions (M_D)	Number of levels (M_L)	Number of symbols $M=(M_L)^{M_D}$	Spectral efficiency $\eta_f.L$ [bit s^{-1} Hz^{-1}]	E_b/N_0 @ $P_b = 10^{-6}$ [dB]	MD-SO-WCDMA SNR gain [dB]
4D-SO-WCDMA	4	2	16	4	10.53	4.15
16-QAM-WCDMA	2	4	"	"	14.68	
8D-SO-WCDMA	8	2	256	8	10.53	13.5
256-QAM-WCDMA	2	16	"	"	24.03	
12D-SO-WCDMA	12	2	2^{12}	12	10.53	23.81
2^{12}-QAM-WCDMA	2	2^6	"	"	34.34	
16D-SO-WCDMA	16	2	2^{16}	16	10.53	34.61
2^{16}-QAM-WCDMA	2	2^8	"	"	45.14	

code-position-modulated (CPM), by independent sets of four (or more) parallel binary symbol streams per CSS. (The optional addition of a CPM modulation scheme falls outside the scope of this paper.)

The proposed new spectrally and power efficient families of SO-CE-GCL-CSS are derived from the zero-cross-correlation (ZCC) sequences proposed in ref. 6, by applying a non-linear root-of-unity-filtering technique presented in ref. 5. By applying the RUF process to any GCL family of sequences,[4] a novel constant-envelope (CE) minimum (Nyquist) bandwidth family is produced which retains the unique correlation properties of the family it was derived from ref. 7. The use of the new families of SO-CE-GCL-CSS requires a synchronous, or at least a quasi-synchronous, communication scenario in both the down- and up-links of the wireless access system – hence the use of the term quasi-synchronous (QS) in the title of the proposed new modulation scheme. The accuracy of the synchronisation system and the maximum delay spread that can be tolerated are primarily functions of the cell size and the geometry of the environment that affects the RF propagation characteristics. The maximum allowable delay or multipath spread that can be accommodated in an operational environment is determined by the characteristics of the periodic auto-correlation function (PACF) of the proposed new family of spreading sequences[6,7] and is typically limited to a few chips of the spreading sequences employed.

MD-SO-WCDMA modem transmitter description

The generation of the 4D-SO-WCDMA output signal $s_l(t)$ may be best described as the sum of sets of four ±1 Volt NRZ binary symbol streams $\{d_{l,m}(t)\}$; $m = 1, 2, 3, 4$ in parallel, each phase modulating the lth orthogonal base $\{\Psi_{l,m}(t)\}$, $m = 1, 2, 3, 4$; $l = 1, 2\cdots M_F$, where the individual $\Psi_{l,m}(t)$ is formed by combinations of products of the perfectly orthogonal real and imaginary parts of the lth CSS, $CSS_l(t) = C_{l,r}(t)+j.C_{l,i}(t)$ from a family of M_F SO-CE-GCL-CSS, and the in-phase and quadrature components of a quadrature carrier, $\{\cos(\omega_c t), -\sin(\omega_c t)\}$, according to:

$$s_l(t) = \sum_{n=-\infty}^{\infty}\left[\left\{d_{l,1}(t')C_{l,r}(t') + d_{l,2}(t')C_{l,i}(t')\right\}\cos(\omega_c t) - \left\{d_{l,3}(t')C_{l,r}(t') + dl,_4(t')C_{l,i}(t')\right\}\sin(\omega_c t)\right] = \frac{\sqrt{T_s}}{2}\sum_{n=-\infty}^{\infty}\left[\sum_{m=1}^{M_D=4} d_{l,m}(t')\psi_{l,m}(t')\right], \quad (1)$$

where $t'=(t - nT_s)$, T_s denotes the symbol period and $\sqrt{T_s}/2$ is a normalization factor. The $\{\Psi_{l,m}(t)\}$, $I = 1, 2, 3, 4$; where the index l denotes one CSS from a family of M_F complex spreading sequences of length L chips, form an orthonormal base over each symbol period $T_s = 4T_b$, spanning the $M_D = 4$-dimensional Euclidian space, with T_b the bit period. The data throughput rate of one basic 4D-SO-WCDMA building block is twice that of a QPSK DSSS modulation system, yielding a spectral efficiency of 4/L [bit s^{-1} Hz^{-1}], i.e. equal to that of $M = 16$-QAM, but with the BER performance of BPSK/QPSK, if identical spreading sequence lengths L and equal spreading bandwidths B_s are assumed. It is straightforward to show that the 4D-SO-WCDMA building block depicted in Fig. 1 may be extended to more dimensions ($M_D > 4$) by adding more super-orthogonal 4D-blocks in parallel, each using only one additional CSS from a family of M_F CE-GCL-CSS for every quadruple increase in the number of dimensions, to yield the composite MD-SO-WCDMA output signal $s(t) = \sum_{l=1}^{M_F} s_l(t)$. This is achieved while maintaining a QPSK-like BER performance, i.e. with significant SNR advantages compared to M-QAM modulated single carrier and M_C-WCDMA modulation schemes for a given BER-performance, as will be illustrated below (with specific reference to Table 1).

Modem receiver

A block diagram of the corresponding basic QS-4D-SO-WCDMA matched filter (integrate and dump) receiver is depicted in Fig. 2. The received signal, $r(t)$, is split into two branches, quadrature carrier demodulated and low-pass filtered, to remove double frequency carrier components. The resultant demodulated in-phase $w_1(t)$ and quadrature-phase $w_2(t)$ signals are again split into two branches, respectively, before being complex despreaded by the lth CSS, say, $CSS_l(t) = C_{l,1} + jC_{l,2}$, from a family of M_F SO-CE-GCL-CSSs. The outputs $\{f_m(t)\}$, $m = 1, 2, 3, 4$ from the complex despreader are then subject to integrate-&-dumped (I&D), to yield outputs $\{g_m(t)\}$, $m = 1, 2, 3, 4$, which are then optimally sampled to produce the decision variables $\{h_m(t)\}$, $m = 1, 2, 3, 4$. Finally, estimates of the original four serial-to-parallel converted symbol streams $\{d_m(t)\}$, $m = 1, 2, 3, 4$, depicted in Fig. 1, are obtained through binary decision devices with thresholds set to zero, to produce the final symbol estimates, $\{\hat{a}_m(t)\}$, $m = 1, 2, 3, 4$. Note that the combination of the quadrature demodulation and complex despreading is equivalent to despreading with an SO base $\{\Psi_{l,m}(t)\}$, $m = 1, 2, 3, 4$, associated with the lth CSS from the family of M_F CSS, i.e. the inverse of the complex spreading process depicted in Fig. 1. Note also the simplicity of the basic QS-4D-SO-WCDMA receiver, and particularly the absence of a complex MUI-cancellation device as a result of the use of families of SO-CE-GCL-CSS in the spreading process. More attention may therefore be focused on synchronization and the incorporation of a complex RAKE processor to exploit any form of inherent multipath diversity in the received WCDMA signal $r(t)$. Details of the latter processor may be found in ref. 16.

Perfect carrier and symbol timing recovery is assumed in this paper—details of high-performance carrier synchronization

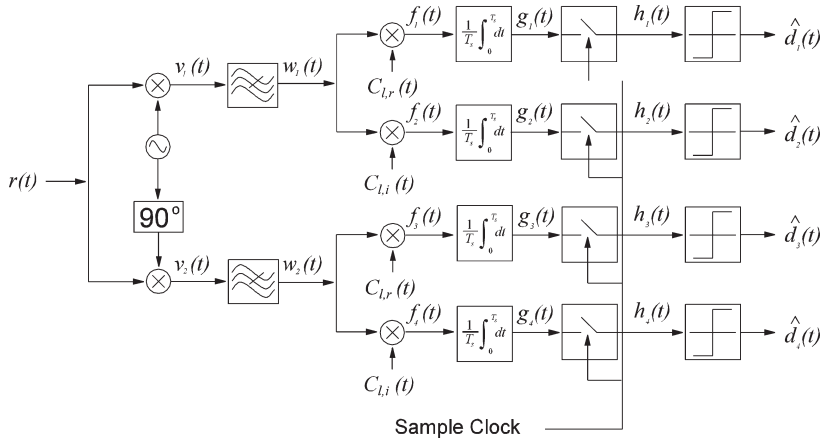

Fig. 2. Correlation-type QS-4D-SO-WCDMA receiver block diagram.

and the complex code-lock-loop (CCLL) have been described in detail in ref. 9 and will not be elaborated on here.

QS multi-code MD-SO-WCDMA modem performance analysis

BER performance in AWGN

We now demonstrate that the uncoded BER performance of the proposed MD-SO-WCDMA configuration remains BPSK/QPSK-like with increasing dimensions M_D, by virtue of the super-orthogonality among the spreading sequences of the family proposed in ref. 7.

Let M_L denote the number of symbol levels per dimension, M_D. In the following discussion, it is also assumed that both the spreading bandwidth and the spreading sequence length L are fixed. The WCDMA processing gain (PG) is defined as the ratio of the chip rate to the symbol rate. Then, the total number of symbols M and the corresponding number of bits per symbol K is given by

$$M = (M_L)^{M_D} = 2^K \quad [symbols] \tag{2}$$

The subsequent analysis is based on the fact that, in general, the MD-SO-WCDMA signal constellation is an M_D-dimensional hypercube centred on the origin of the signal space spanned by an orthonormal base such as the one defined in (1).[10] In fact, with $M_D = 4$ and $M_L = 2$, $M = 2^{M_D} = 16$ symbols are situated on the vertices of an $M_D = 4$-dimensional hypercube, where the number of bits per symbol equals $K = M_D = 4$. The latter relationship is a characteristic of an M_D-dimensional hypercube. Note that each dimension of the MD-SO-WCDMA signal space only carries one bit of information, i.e. according to (1), the MD-SO-WCDMA modulator only performs binary ($M_L = 2$) modulation of GCL CSS per dimension. Furthermore, the coordinates of nearest-neighbour symbols differ only in one bit position, that is, the signal constellation exhibits a natural Gray mapping of bits onto symbols.

We now proceed with the MD-SO-WCDMA BER-analysis in AWGN. It is well known from ref. 11 that the correlation ρ_r amongst all adjacent pairs of symbols in the M_D-dimensional hypercube signal space is given by:

$$\rho_r = \frac{M_D - 2}{M_D} \quad . \tag{3}$$

Furthermore, using (3), the Euclidean distance between nearest-neighbour symbols can be shown to be:

$$d = \sqrt{2E_s(1-\rho_r)} = \sqrt{\frac{4E_s}{M_D}} \quad . \tag{4}$$

Since the symbol energy equals $E_s = M_D.E_b$, with E_b the energy per bit, d simplifies to $\sqrt{4E_b}$, and the symbol error rate (SER) of the MD-SO-WCDMA modulation scheme in AWGN is approximated by:[10,11]

$$P_{M_D} = \left[1-(1-P_2)^{M_D}\right] = 1-\left(1 - M_D P_2 + \frac{M_D(M_D-1)P_2^2}{2!} - \cdots + P_2^{M_D}\right)$$
$$\approx M_D P_2 \quad iff \quad M_D \geq 4 \ \ and \ \ P_2 << 1. \tag{5}$$

where P_2 denotes the pair-wise symbol error between adjacent (nearest-neighbour) symbols at distance d, given by:

$$P_2 = Q\left[\sqrt{\frac{d^2}{2N_0}}\right] , \tag{6}$$

with d defined in (4). In (6), N_0 denotes the one-sided noise power spectral density, and Q the well-known Gauss tail probability, defined as $Q(x) = \frac{1}{\sqrt{2\pi}}\int_x^\infty e^{-\frac{y^2}{2}}dy$. Now, when $M_D \geq 4$ and $P_2 << 1$, Equation (5), with a high degree of accuracy, simplifies to

$$P_{M_D} \approx M_D P_2 = M_D\, Q\left[\sqrt{\frac{4E_s}{2M_D N_0}}\right] = M_D\, Q\left[\sqrt{\frac{2E_b}{N_0}}\right] \quad . \tag{7}$$

By virtue of the Gray bit-encoding of nearest-neighbour symbols, the bit error rate in AWGN is well approximated by

$$P_b \approx \frac{1}{M_D} P_{M_D} = P_2 = Q\left[\sqrt{\frac{2E_b}{N_0}}\right] \quad . \tag{8}$$

Note that (8) is independent of the number of dimensions M_D. This implies that the BER of the proposed new QS-MD-SO-WCDMA modulation scheme remains QPSK-like as $M_D \to \infty$, the only requirement being that a set of *super-orthogonal* CSS be employed, such as the family presented in ref. 7, or the extended-orthogonal (EO) sequences proposed in ref. 12. The primary implication of this is that the overall data throughput rate, and thus, the spectral efficiency (given a fixed spreading bandwidth), may be doubled (compared to QPSK) for every doubling of the number of dimensions, $M_D = 4$. Moreover, the latter may be achieved by simply adding basic $M_D = 4$-dimensional SO-WCDMA building blocks in parallel, using one new distinct CSS for each new set of $M_D = 4$ dimensions, the only limitation being the available family size M_F (i.e. the number of available CSS in a given set of SO-CSS). The resulting composite

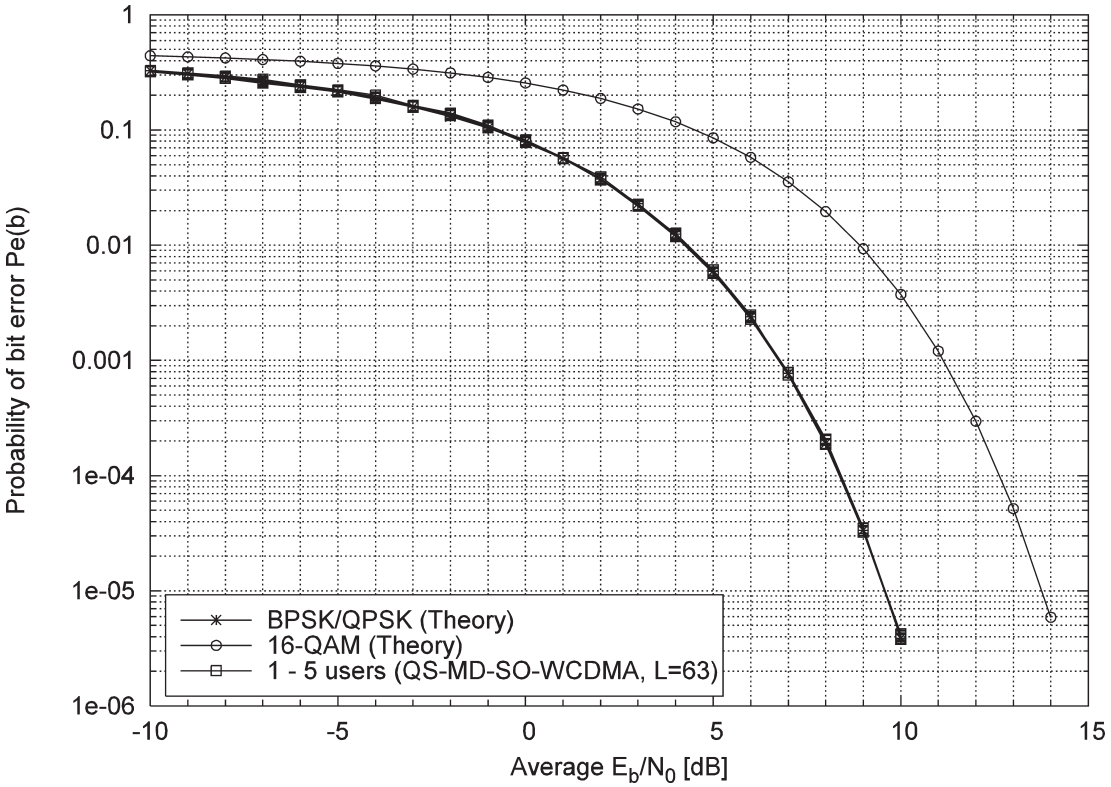

Fig. 3. Simulated uncoded BER performance graphs in AWGN for 4D- to 20D-SO-WCDMA, compared to 2D-QPSK WCDMA and 16-QAM WCDMA. The former MD-SO-CDMA systems facilitate data throughputs of 2 to 10 times 2D-QPSK WCDMA, and 1 to 5 times 16-QAM WCDMA, respectively, given identical spreading sequence lengths L and Nyquist filtered ($\alpha = 0$) spreading bandwidths, B_s.

multi-code (MC) modulator is called a MC-MD-SO-WCDMA modem. Consequently, generic upwards-expandability of the basic generic 4D-SO-WCDMA modulator may be achieved, while maintaining QPSK-like BER performance in AWGN as the data throughput linearly increases (doubles) with the addition of each new set of $M_D = 4$ dimensions and one additional new CSS from the family of GCL-SO-CSS for each quadruple increase of dimensions.

Equation (8) is verified and confirmed in Fig. 3, depicting the BER performance for $M_D = 4$ to $M_D = 20$-dimensional QS-MD-SO-WCDMA modulators in AWGN (the latter comprises $5\,M_D = 4$-dimensional building blocks in parallel). Note, for example, that the data throughputs of the $M_D = 4$ to $M_D = 16$ QS-MD-SO-WCDMA modulation schemes corresponds to the $M_D = 2$-dimensional $M = 2^{K=4} = 16$ to $M = 2^{K=16}$ QAM modulated single carrier WCDMA modulators, i.e. 2 to 8 times that of QPSK, given identical spreading sequences lengths and bandwidths, where M and K are defined in (2). However, this is achieved by QS-MD-SO-WCDMA while maintaining the BER performance of QPSK, signifying a huge performance advantage over M-QAM single carrier and multi-carrier WCDMA modulation schemes when $M \geq 16$ (or $M_L \geq \sqrt{M} = 4$).

A performance comparison between QS-MD-SO-WCDMA and M-QAM modulated WCDMA modulation schemes is presented in Table 1. The table lists various MD-SO-WCDMA schemes, together with an equivalent M-QAM WCDMA modulation scheme with identical normalized (with the spreading factor L) spectral efficiencies, $\eta_f L$ [bits s^{-1} Hz^{-1}], where L is identical for all modulation schemes considered.

The spectral efficiencies are calculated in a double-side-band (DSB) spreading bandwidth B_s, assuming a Nyquist filtered output frequency spectrum with spectral roll-off factor α approaching zero.

This table demonstrates, for example, that the new basic 4D-SO-WCDMA modulation scheme requires approximately 4 dB less E_b/N_o to achieve a BER of 10^{-6} than M = 16-QAM modulated high data rate (HDR) WCDMA in AWGN, for identical data throughputs and equal spreading bandwidths. Furthermore, the BPSK/QPSK-like BER performance of the $M_D \geq 4$ SO-WCDMA modulators are achieved with insignificant performance degradation when operating at the 1 dB saturation point of the power amplifier (PA) (and beyond), due to the near constant instantaneous power outputs of these modulators, even for $M_D \geq 4$. The latter has been confirmed with extensive peak-to-average-power ratio cumulative complementary distribution function (PAPR-CCDF) power amplifier saturation measurements in ref. 14.

BER performance analysis in a Nakagami-fading multipath channel

The theoretical BER for uncoded QS-4D-SO-WCDMA (without CPM) in fading multipath conditions also follows from the expression in (5). This yields, after inserting the expression for the SER of a MD-QPSK modulation technique in a Rayleigh fading channel with L_m independent multipaths, with or without an adaptive RAKE receiver with $L_r = L_m$ active taps:[6,15]

$$P_b \approx \frac{2}{\log_2 M}\sqrt{\frac{\gamma_s}{1+\gamma_s}}\,\frac{(1+\gamma_s)^{-e_s}\,\Gamma\left(e_s+\frac{1}{2}\right)}{\sqrt{\pi}\,(e_s+1)}\cdot {}_2F_1\left\{1, e_s+\tfrac{1}{2}; e_s+1; \frac{1}{1+\gamma_s}\right\} \qquad (9)$$

where $\gamma_s = \left(\frac{\gamma_m \Omega_s}{2 e_s}\right)$, $\gamma_m = \gamma \sin^2\left(\frac{\pi}{M}\right)$, $\gamma = \frac{E\Omega_0}{N_0}$ and $E = PLT_c$, with P the symbol power, L the spreading sequence length, and T_c the chip period. In (9), the natural Gray mapping of bits onto adjacent symbols in the QS-4D-SO-WCDMA signal constellation has been used to obtain an approximation of the BER, P_b, given the

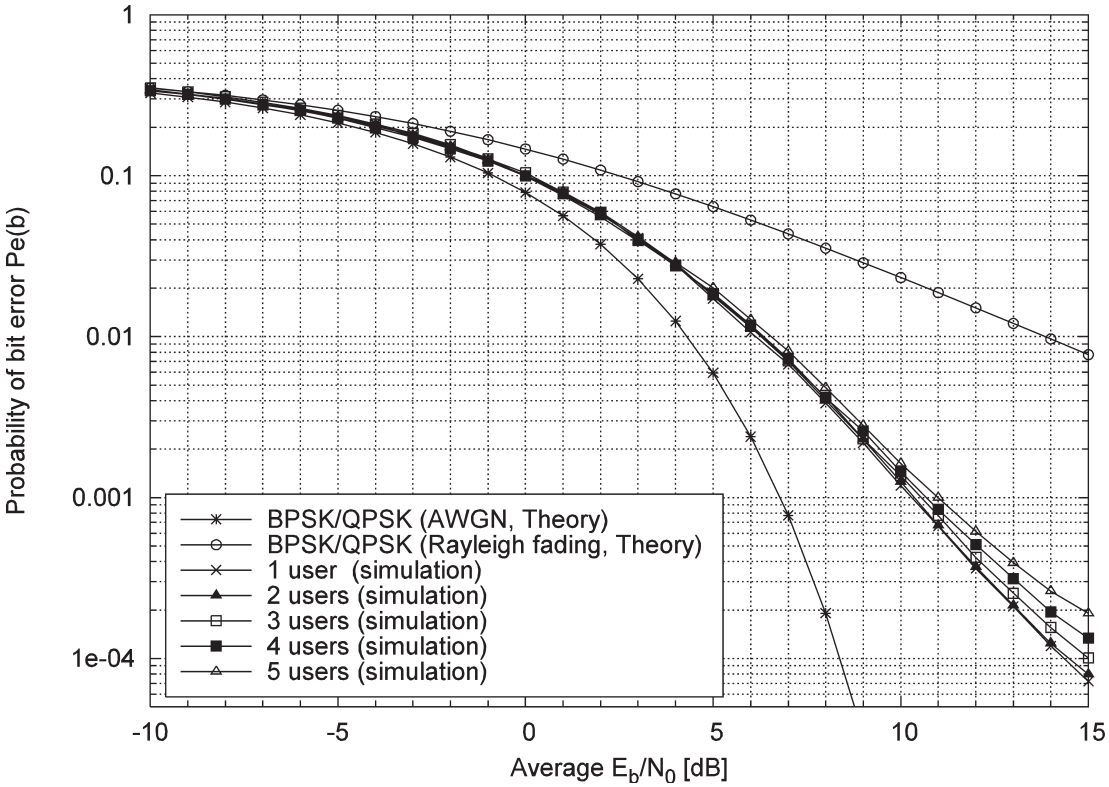

Fig. 4. Uncoded BER performance of QS-4D-SO-WCDMA employing SO-CE-GCL-CSS of length $L = 63$ in an exponentially weighted multipath Rayleigh fading channel with an initial Ricean and two statistically independent Rayleigh fading multipaths (see ref. 16, pp. 95–98 for details).

expression of the symbol error rate, P_M. ${}_2F_1\{a,b;c;z\}$ denotes the confluent hyper-geometric function and $\Gamma(\cdot)$ the Gamma function. Note also that $\Omega_l^{(k)} = \Omega_0^{(k)} e^{-\delta l}$ is the second moment of $\rho_l^{(k)}$, where $\Omega_0^{(k)}$ represents the second moment of the initial path strength of the kth user. The variable $\delta \geq 0$ denotes the rate of exponential decay of the multipath intensity profile of the channel. The $\{\rho_l^{(k)}\}$ are independent identically distributed (iid) Nakagami random variables. Also, $e_s = p\dfrac{q^2(L_r,\delta)}{q(L_r,2\delta)}$, and $\Omega_s = q(L_r, \delta)$, with $q(a,b) = 1 - e^{-ab})/(1 - e^{-b})$.The variable p is a positive real number, such that $1/p$ gives an indication of the 'fading figure' of the channel.[15]

Figure 4 depicts the uncoded performance of the said QS-MD-SO-WCDMA modulators with $M_D = 4$ to $M_D = 20$ in an exponentially-weighted three-path channel consisting of an initial Rician fading path, followed by two smaller exponentially weighted independently Rayleigh fading paths, *without* a complex RAKE processor in the receiver. The results are obtained for k = 1–5 (maximum 7) simultaneous users, with spreading sequences allocated from families of SO-CE-GCL-CSS[7] of length $L = 63$. Details of the experimental setup, and particularly the fading multipath channel, may be found in ref. 16. The BER-graphs for the AWGN and flat Rayleigh fading channels are also depicted, representing lower and upper performance bounds, respectively. Using the MUI-free family of CSS, results in an approximate 13–14 dB performance advantage over a single-user flat fading system, and a performance loss of only approximately 3.5 dB compared to the single-user AWGN bound at a BER of $P_b = 10^{-3}$, signifying a virtually MUI-free receiver. Note also that there is a small deterioration in BER with an increase in the number of users for average signal-to-noise ratio per bit values exceeding E_b/N_o = 10 dB, i.e. for BER values below 10^{-3}. This asymptotic error rate plateau phenomenon may be attributed to the presence of multipath and the absence of a RAKE multipath combining processor, as is verified by the results presented in Fig. 5.

Figure 5 repeats the foregoing analysis on RUF families of CE-GCL Zadoff-Chu (ZC)[13] and SO-CE-GCL-CSS[7] spreading sequences, respectively, *with* the presence of a complex L_r = 3-finger RAKE processor in the receiver.[16] The theoretical BER graph obtained from (9) is also included for references purposes. The performance degradation of the non-ideal (i.e. not perfectly orthogonal) system employing ZC CE-GCL-CSS,[13] compared to the essentially MUI-free performance of the modem with multiple users using spreading sequences from the family of SO-CE-GCL-CSS, is immediately evident. This degradation is attributed to the cross-correlation interference between users employing CSS from a family of non-super-orthogonal RUF Zadoff-Chu CE-CSS of length $L = 63$, causing substantial MUI. Compared to the corresponding results in Fig. 4, it is noted that the incorporation of a complex RAKE processor has definitely reduced the BER degradation as a result of an increase in the number of users, as well as at least partly eradicated some of the asymptotic BER error rate plateau phenomenon observed in Fig. 4 for E_b/N_o beyond 10 dB and P_b below 10^{-3}. The latter graph corresponds very well with the theoretical result defined in (9), the simulated results being within 1 dB of theory. The use of SO-CE-GCL-CSS therefore practically obviates the need for sophisticated MUI-cancellation techniques in the proposed new 4D-SO-WCDMA modem, yielding a significantly simplified receiver and a suitable platform on which notable performance gains can be achieved through the incorporation of appropriate forward error correction (FEC) techniques.

Conclusion

A high-performance power and spectrally efficient novel single carrier QS-4D-SO-WCDMA modem building block has been presented as an alternative to M-QAM single carrier and multi-carrier modulated OFDM and CDMA modulation

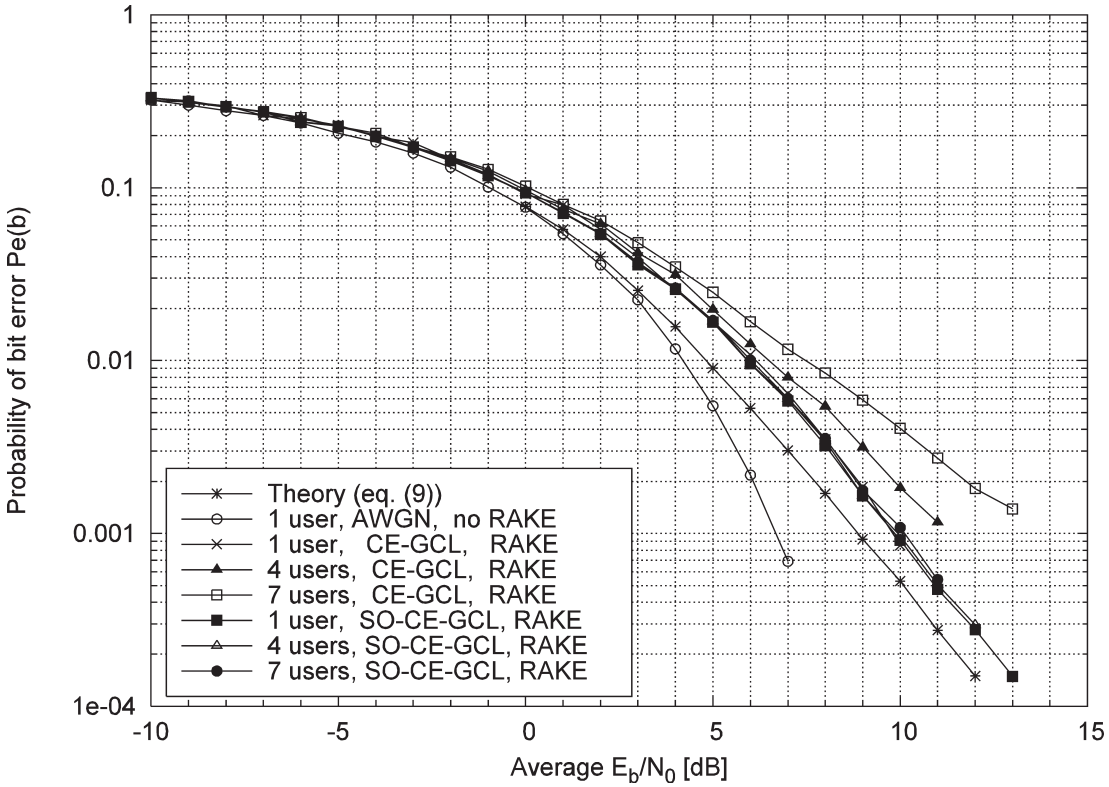

Fig. 5. BER performance of QS-4D-SO-WCDMA SO-CE-GCL-CSS versus CE-GCL (Zadoff-Chu) sequences of length $L = 63$ in a multipath Rayleigh fading channel with $L_m = 3$ paths (one Rician and two statistically independently Rayleigh fading), with a complex RAKE receiver processor with $L_r = 3$ active fingers. The single-user AWGN-bound (without RAKE) and the theoretical result of Equation (9) are included for reference purposes.

standards employed in 3G or to be employed in next generation (4G) wireless access systems. It has been shown in ref. 14 that the proposed QS-MD-SO-WCDMA modem can operate close to the 1 dB PA saturation point, with typically 3–6 dB less PA back-off than existing M-QAM modulated M_c-OFDM and M_c-CDMA modulation schemes. This signifies a notable communication range advantage, or alternatively, significantly improved handset battery life for a given performance level and range compared to existing methods. Notable MUI-free BER performance advantages have been demonstrated using a family of SO-CE-GCL-CSS,[7] compared to conventional (Zadoff-Chu) CE-GCL-CSS,[13] in both AWGN (Fig. 3) and multipath fading channels (Figs 4 and 5), with and without RAKE maximum ratio combining (MRC). The MUI-free advantages are achieved with a low-complexity matched filter correlation-type receiver, without the need for complex MUI-mechanisms, but with the possible inclusion of RAKE MRC processing to exploit the presence of inherent multipath diversity, as well as appropriate FEC techniques to yield performance gains approaching the single-user and even the Shannon bound.

The combination of the proposed new MD-WCDMA architecture with families of SO-CE-GCL-CSS renders a unique combination of spectral occupancy (i.e. minimum Nyquist bandwidth) and exceptional power efficiency by virtue of the constant envelope (instantaneous output power), with data throughputs doubling with the addition of each parallel basic 4D-WCDMA building block, while simultaneously maintaining the BER performance of BPSK/QPSK in both AWGN and Rayleigh fading multipath channels. The virtues of the proposed new MD-SO-WCDMA modulation schemes make it an attractive alternative for next generation wireless access and WLAN applications.

The authors are grateful to Jacques van Wyk and Frans Marx for their assistance with the processing of some of the diagrams and results presented in this paper. The support of the Centre for Radio and Digital Communication (CRDC), as well as financial support by the National Research Foundation through their Information and Communication Technology (ICT) Programme, under the project title 'IP-based rural communication system' (GUN 2053415), is also acknowledged.

Recieved 26 April 2006. Accepted 24 October 2007.

1. Choi B.J., Kuan E.L. and Hanzo L. (1999). Crest-factor study of MC-CDMA and OFDM. In *IEEE Vehicular Technology Conference* (*VTC'99*), pp. 233–237.
2. Davis J.A. and Jedwab J. (1999). Peak-to-mean power control in OFDM, Golay complementary sequences and Reed-Muller codes. *IEEE Trans. Information Theory* **45**(7), 2397–2417.
3. Rössing C. and Tarokh V. (2001). A construction of OFDM 16-QAM sequences having low peak powers. *IEEE Trans. Information Theory* **47**(5), 2091–2097.
4. Popović B.M. (1992). Generalized Chirp like polyphase sequences with optimum correlation characteristics. *IEEE Trans. Information Theory* **IT-38**(4), 1404–1409.
5. Lötter M.P. and Linde L.P. (1995). Constant envelope filtering of complex spreading sequences. *Electron. Lett.* **31**, 1406–1407.
6. Park S.I., Park S.R., Song I. and Suehiro N. (2000). Multiple-access interference reduction for QS-CDMA systems with a novel class of polyphase sequences. *IEEE Trans. Information Theory* **46**, 1448–1458.
7. Linde L.P., Pryra I. and Swanepoel S.A. (2003). On a new family of complex spreading sequences with zero cross-correlation properties. *Trans. S. Afr. Inst. Electr. Engnrs* **94**, 50–56.
8. Scaglione A., Giannakis G.B. and Barbarossa S. (2000). Lagrange/Vandermonde MUI eliminating user codes for quasi-synchronous CDMA in unknown multipath. *IEEE Trans. Signal Processing* **48**(7), 2057–2073.
9. Marx F.E. (2005). *DSSS communication link employing complex spreading sequences.* M.Eng dissertation, University of Pretoria, South Africa.
10. Wozencraft J.M. and Jacobs I.M. (1965). *Principles of Communication Engineering,* chap. 4, pp. 254–257. Wiley, New York.
11. Proakis J.G. (2001). *Digital Communications,* 4th edn. McGraw-Hill, New York.
12. Lu L. and Dubey V.K. (2004). Extended orthogonal polyphase codes for multicarrier CDMA systems. *IEEE Commun. Lett.* **8**(12), 700–702.
13. Chu D.C. (1972). Polyphase codes with good periodic correlation properties. *IEEE Trans. Information Theory* **18**(4), 531–532.
14. Linde L.P. and Marx F.E. (2003). Power and spectral efficiency performance of a family of WCDMA-modulated constant-envelope root-of-unity filtered complex spreading sequences in non-linear power amplification. *Trans. S. Afr. Inst. Electr. Engnrs* **94**(4), 57–67.
15. Eng T. and Milstein L.B. (1995). Coherent DS-CDMA performance in Nakagami multipath fading. *IEEE Trans. Commun.* **43**, 1134–1143.
16. Staphorst L. (2005). In *Viterbi decoded linear block codes for narrowband and wideband communication over mobile fading channels,* pp. 95–98. M.Eng. dissertation, University of Pretoria, South Africa.